Effects of acyl chain length, unsaturation, and pH on thermal stability of model discoidal HDLs[s]

Madhumita Guha, Donald L. Gantz, and Olga Gursky[1]

Department of Physiology and Biophysics, Boston University School of Medicine, Boston MA 02118

Abstract   HDLs prevent atherosclerosis by removing excess cell cholesterol. Lipid composition affects HDL functions in cholesterol removal, yet its effects on the disk stability remain unclear. We hypothesize that reduced length or increased cis-unsaturation of phosphatidylcholine acyl chains destabilize discoidal HDL and promote protein dissociation and lipoprotein fusion. To test this hypothesis, we determined thermal stability of binary complexes reconstituted from apoC-I and diacyl PCs containing 12–18 carbons with 0–2 cis-double bonds. Kinetic analysis using circular dichroism shows that, for fully saturated PCs, chain length increase by two carbons stabilizes lipoprotein by $\delta\Delta G^*$ (37°C) $\cong$ 1.4 kcal/mol, suggesting that hydrophobic interactions dominate the disk stability; distinct effects of pH and salt indicate contribution of electrostatic interactions. Similarly, apoA-I-containing disks show increased stability with increasing chain length. Acyl chain unsaturation reduces disk stability. In summary, stability of discoidal HDL correlates directly with fatty acyl chain length and saturation: the longer and more fully saturated are the chains, the more extensive are the stabilizing lipid-protein and lipid-lipid interactions and the higher is the free energy barrier for protein dissociation and lipoprotein fusion. This sheds new light on the existing data of cholesterol efflux to discoidal HDL and suggests that moderate lipoprotein destabilization facilitates cholesterol insertion.—Guha, M., D. L. Gantz, and O. Gursky. **Effects of acyl chain length, unsaturation, and pH on thermal stability of model discoidal HDLs.** *J. Lipid Res.* **2008.** 49: 1752–1761.

Cardioprotective action of HDLs results, in part, from their central role in cholesterol removal from peripheral tissues to the liver via reverse cholesterol transport (RCT) (1, 2). During RCT, HDLs are remodeled by plasma factors and form distinct subclasses differing in particle size, composition, structure, and functions (3, 4). Nascent HDLs form discoidal particles comprised of a phospholipid bilayer containing variable amounts of free (unesterified) cholesterol and proteins (apolipoproteins) that adopt a belt-like α-helical conformation around the particle perimeter (**Fig. 1**) (5, 6). These discoidal HDLs and their lipid-poor precursors stimulate cholesterol efflux from peripheral cells, including arterial macrophages. Cholesterol-containing disks are converted by LCAT into mature spherical HDLs, with apolar lipids (mainly cholesterol esters) sequestered in the core and proteins and polar lipids [mainly phosphatidyl cholines (PC) and free cholesterol] forming the particle surface. Upon further action of LCAT or lipid transport proteins, these small spherical HDL_3 fuse into larger HDL_2 particles that deliver their cargo of cholesterol esters to the liver. Lipid-poor apolipoprotein A-I (apoA-I), the major HDL protein, dissociates upon HDL fusion and provides an efficient acceptor of cell cholesterol and PCs, eventually entering the pool of discoidal HDL (7). The focus of this work is on the effects of PC fatty acyl chain composition on the stability and remodeling of discoidal HDL.

Changes in surface lipid composition can modulate HDL functions via several mechanisms (8). First, the ensuing conformational changes in surface proteins and lipids may directly impact HDL interactions with lipoprotein receptors, lipid transport proteins, and lipolytic enzymes at key junctures of RCT. Second, changes in physical properties of surface lipids (such as packing defects and fluidity) may affect cholesterol and protein insertion into, or dissociation from, this surface during RCT. Third, changes in the amount and composition of surface lipids may affect particle fusion, which is an important step in metabolic HDL remodeling (3, 7). Lipid composition may also affect stability of HDL assembly, thereby altering the rate of

Abbreviations: apo, apolipoprotein; CD, circular dichroism; DLPC, dilauroyl PC; DMPC, dimyristoyl PC; DPPC, dipalmitoyl PC; DSC, differential scanning calorimetry; DSPC, distearoyl PC; EM, electron microscopy; PC, phosphatidylcholine; PLPC, palmitoyl-linoleoyl PC; POPC, palmitoyl-oleoyl PC; RCT, reverse cholesterol transport; rHDL, reconstituted HDL; T-jump, temperature jump.

[1] To whom correspondence should be addressed.

    e-mail: Gursky@bu.edu

[s] The online version of this article (available at http://www.jlr.org) contains supplemental data in the form of four figures.
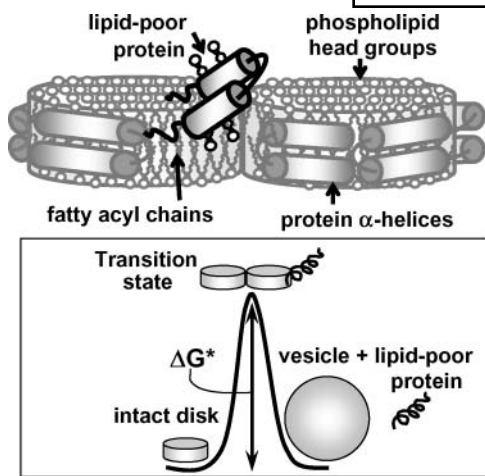
Fig. 1. Cartoon illustrating denaturation of discoidal HDL. Free energy diagram shows rate-limiting transition state that separates reconstituted HDL (rHDL) in their native (disks) and denatured states (protein-containing vesicles and dissociated lipid-poor protein). It involves transient disruption of protein and lipid packing interactions and solvent exposure of apolar moieties during protein dissociation and lipoprotein fusion. Kinetic free energy of lipoprotein stability, $\Delta G^* = G(\text{transition}) - G(\text{native})$, is indicated.

metabolic HDL remodeling and/or shifting the population distribution among HDL subclasses. Reconstituted HDLs (rHDLs) of controlled composition provide useful experimental models for studying these effects (8, 9). They enable us to assess, one by one, how changes in the constituent apolipoproteins (size, hydrophobicity, secondary structure) and lipids (PC composition, cholesterol content, etc.) affect HDL structure, stability, and functions (Refs. 8–16 and references therein). Here, we use discoidal rHDL to test the effects of PC acyl chain length and unsaturation on lipoprotein stability and correlate them with the existing functional data.

One of the most detailed studies of the effects of acyl chain composition on rHDL structure and function was the analysis of apoA-I complexes with dimyristoyl PC

(DMPC), dipalmitoyl PC (DPPC), distearoyl PC (DSPC), and their unsaturated analogs by Davidson and et al. (13). The results showed that longer-chain and/or more saturated PCs form less efficient acceptor particles for cholesterol. Also, longer-chain PCs reportedly formed less stable complexes with apoA-I, which was inferred from spectroscopic measurements after rHDL incubation with denaturant (13). Later, we demonstrated that such "end-point" measurements were inadequate for studies of thermodynamically irreversible HDL denaturation, and we developed an alternative kinetic approach for quantitative analysis of lipoprotein stability (17, 18). We showed that the thermodynamically irreversible step in HDL denaturation involves apolipoprotein dissociation and particle fusion that compensates for the ensuing reduction in the surface-to-volume ratio, leading to high free energy barrier, ΔG^*, that maintains HDL stability (Fig. 1). Importantly, HDL perturbations by heating, denaturants, detergents, or plasma factors lead to similar remodeling into dissociated lipid-poor protein and fused particles, suggesting that metabolic HDL remodeling is modulated by similar kinetic barriers that originate from protein dissociation and lipoprotein fusion (18). Here, we apply this kinetic approach to reevaluate the effects of PC acyl chain length and unsaturation on rHDL stability.

We hypothesize that diacyl PCs containing longer and more fully saturated acyl chains form more stable binary complexes with apolipoproteins, that is, have higher kinetic barriers ΔG^* that decelerate protein dissociation and lipoprotein fusion. To test this hypothesis, we analyzed thermal denaturation kinetics of discoidal rHDLs reconstituted from apoC-I and fully saturated diacyl PCs differing in their chain length from 12 to 18 carbons [dilauroyl PC (DLPC), DMPC, DPPC, and DSPC] or their mono- or diunsaturated analogs that are abundant in plasma HDL (19) [palmitoyl-oleoyl PC (POPC) and palmitoyl-linoleoyl PC (PLPC)] (**Table 1**). We used the smallest human apolipoprotein, apoC-I (6 kDa), which is a potent inhibitor of lipoprotein lipase and cholesterol ester transfer protein,

TABLE 1.   Energetic and structural parameters of PCs and their complexes with apoC-I

	Lipids		Discoidal Complexes with ApoC-I			
Name	Acyl chains sn:1, sn:2	T_c, °C[a]	Thickness $<l>$, nm[b]	Diameter $<d>$, nm[c]	Arrhenius Activation Energy E_a, kcal/mol[d]	$\delta\Delta G^*(37°)$, kcal/mol[e]
DLPC	12:0, 12:0	−1	5.4 ± 0.3	17.6 ± 2.2	20 ± 5	−1.4
DMPC	14:0, 14:0	24	5.6 ± 0.3	15.5 ± 2.2	25 ± 5	0.0
DPPC	16:0, 16:0	41	6.1 ± 0.4	16.0 ± 2.2	30 ± 6	+1.5
DSPC	18:0, 18:0	54	6.4 ± 0.4	14.4 ± 3.0	36 ± 6	+2.9
POPC	16:0, 18:1	−5	5.6 ± 0.4	16.5 ± 6.0	20 ± 6	∼0
PLPC	16:0, 18:2	−20	5.5 ± 0.3	14.3 ± 5.0	18 ± 6	−0.2

DLPC, dilauroyl PC; DMPC, dimyristoyl PC; DPPC, dipalmitoyl PC; DSC, differential scanning calorimetry; DSPC, distearoyl PC; PLPC, palmitoyl-linoleoyl PC; POPC, palmitoyl-oleoyl PC. The values of E_a and ΔG^* pertain to mole of cooperative unit involved in rHDL denaturation, which probably comprises one protein and several lipid molecules (see Discussion).

[a] Temperature of gel-to-liquid crystal phase transition in pure PC (20).

[b] STD reflects experimental error in determination of disk thickness from the stacks observed by negative staining EM (such as those in Fig. 2A).

[c] STD reflects heterogeneity in the disk diameters determined by EM.

[d] Determined from the slopes of the Arrhenius plots (Fig. 4D) that were obtained from exponential fitting of the kinetic CD data, $\Theta_{222}(t)$ (such as those in Fig. 2). The accuracy in E_a determination reflects fitting errors and deviations among different data sets.

[e] Difference in free energy of stability at 37°C as compared with apoC-I:DMPC disks. The values were obtained from linear extrapolation of the Arrhenius plots to 37°C (Fig. 4D); the accuracy in $\delta\Delta G^*(37°C)$ is ∼0.2 kcal/mol. For complexes with longer-chain PC (16 to 18 carbons) that show two-phase kinetics, the values for the first kinetic phase (corresponding to fusion of intact disks) are listed.

Acyl chain effects on rHDL stability   1753

a secondary activator of LCAT, and an important modulator of lipoprotein metabolism (21, 22). ApoC-I has high sequence, structural and functional similarity to larger exchangeable apolipoproteins; due to its small size, apoC-I provides a sensitive experimental model for testing the effects of lipoprotein composition and solvent conditions on HDL structure and stability (Refs. 15, 16, 23 and references therein). To test whether the key findings in PC complexes with apoC-I extend to other apolipoproteins, we used similar binary complexes containing human plasma apoA-I. The results support our hypothesis and shed new light on the existing data on cholesterol efflux to discoidal HDL. Our results also provide better insight into the role of hydrophobic and electrostatic interactions in disk assembly and the physical nature of the rate-limiting transition state in HDL remodeling.

MATERIALS AND METHODS

Protein and lipoprotein preparation

Full-size human apoC-I with unblocked termini was synthesized at 21st Century Biochemicals as described (16, 17); peptide amino acid composition and purity (>97%) were confirmed by mass spectrometry and HPLC. Human apoA-I and apoA-II were isolated from single-donor HDLs of healthy volunteer donors and refolded as described (15); protein purity assessed by HPLC was >95%. Lipids (>99% purity) were purchased from Avanti Polar Lipids; sodium cholate was from Sigma. Unless otherwise stated, the buffer used throughout this work was 5 mM Na phosphate, pH 7.7.

Discoidal protein:lipid complexes were reconstituted by cholate dialysis (8, 9). To verify that disk diameters did not significantly affect disk stability, binary complexes that had similar protein and lipid composition (DMPC, DPPC, DSPC) but distinctly different diameters were obtained and characterized (see supplementary Figs. III and IV).

Negative staining EM

Protein-lipid complexes were visualized at 22°C by negative staining electron microscopy (EM) using a CM12 transmission electron microscope (Philips Electron Optics) as described (17). Particle size analysis was carried out in EXCEL using 200–300 particles per image.

CD spectroscopy

Circular dichroism (CD) data were recorded using AVIV-400 or AVIV-62DS spectrometers with thermoelectric temperature control. Far-ultraviolet CD spectra and kinetic and melting data were recorded from lipoprotein samples of 20–30 μg/ml protein concentrations. In kinetic temperature-jump (T-jump) experiments, the sample temperature was rapidly increased at time t = 0 from 25°C (for DMPC, DPPC, and DSPC complexes) or from 4°C (for DLPC complexes, which were unstable at 25°C) to higher temperatures; the time course of protein unfolding was monitored at 222 nm. Importantly, the T-jump data recorded from DMPC-containing disks did not depend on the starting temperature (4–26°C). Hence, the results of our kinetic studies were independent of the initial state of lipid (gel or liquid crystal). In the melting experiments, CD data were recorded at 222 nm upon sample heating and cooling with 1°C increment at a scan rate of 80 or 11°C/h. Following the baseline subtraction, the CD data were normalized to protein concentration and expressed as molar residue ellipticity, $[\Theta]$. Protein α-helical content was determined from the CD measured at 222 nm, $[\Theta]_{222}$, as described (17).

Kinetic analysis

The T-jump CD data were analyzed by using an Arrhenius model as described (17). Kinetic data recorded at each temperature were approximated by multiexponentials: $[\Theta]_{222}(t) = A_1 \exp(-t/\tau_1) + A_2 \exp(-t/\tau_2) +$

Here, A_1 and A_2 are the amplitudes of the kinetic phases, and τ_1 and τ_2 are the exponential relaxation times that are inverse of the reaction rates, $k = 1/\tau$. The activation energy $E_a \cong \Delta H$ for each kinetic phase was determined from the slope of the Arrhenius plot, $-RT \ln k(T)$ versus $1/T$. Changes in the Gibbs free energy of the kinetic disk stability, ΔG^*, resulting from changes in lipid composition or solvent conditions were determined from the shifts in the Arrhenius plots, $\delta \Delta G^*(T) = -RT \delta[\ln k(T)]$. The values of E_a and ΔG^* determined from the spectroscopic rate measurements pertain to mole of cooperative unit involved in the transition (see Discussion).

Differential scanning calorimetry

DSC data (courtesy of Dr. Shobini Jayaraman) were recorded using an upgraded MC2 instrument (Microcal) from binary complexes of apoA-I or apoA-II with fully saturated diacyl PCs. The disk samples (1.5–2 mg/ml protein in 5 mM Na phosphate buffer, pH 7.7) were heated from 5–100°C at a constant rate of 90°C/h, and heat capacity data $C_p(T)$ were recorded. Following buffer baseline subtraction, the data were normalized to protein concentration.

All experiments in this study were repeated three to eight times to ensure reproducibility.

RESULTS

Structural parameters of rHDL

Freshly prepared rHDLs were observed at 22°C by negative staining EM (Fig. 3A and supplemental Fig. I). All lipids formed discoidal complexes with apoC-I that were observed face-up or stacked on edge. The disk thickness estimated from the stacks ranged from 5.4 ± 0.3 nm for DLPC to 6.4 ± 0.4 nm for DSPC (Table 1) and was consistent with the expected increase by ~0.3 nm per two CH_2 groups for fully saturated acyl chains in a bilayer conformation. The disk diameters varied from 11–19 nm, with the mean value ranging from <d>=17.6 nm for DLPC to 14.4 for DSPC (Table 1). The results of our earlier (16, 24, 25) and current studies using binary complexes of proteins and lipids (DMPC, DPPC, DSPC) consistently show that such diameter variations have no significant effect on thermal stability of the disks measured in the melting or kinetic T-jump experiments (supplementary Figs. III and IV). Far-ultraviolet CD spectra of the apoC-I-containing complexes were similar (17) but showed a small gradual increase in the α-helical content from approximately 61% to 68% upon chain length increase from 12 to 18 carbons.

Thermal denaturation kinetics of apoC-I:DPPC complexes

Lipoprotein stability was quantified by monitoring the time course of protein unfolding in T-jumps. **Fig. 2A** shows
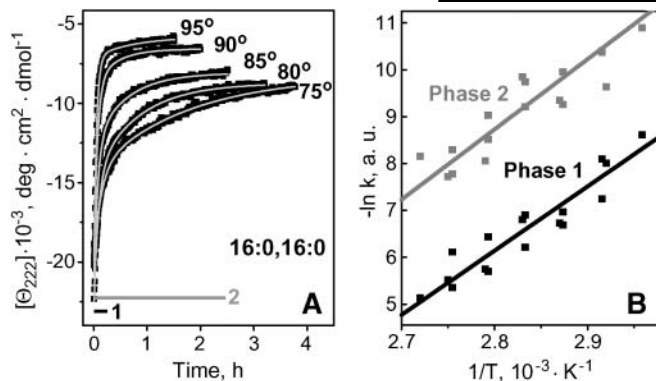
Fig. 2. Thermal denaturation kinetics of apoC-I:DPPC complexes. Buffer conditions are 5 mM Na phosphate, pH 7.7. A: Kinetic circular dichroism (CD) data, $\Theta_{222}(t)$, were recorded from intact disks in T-jumps from 25°C to higher temperatures (as indicated). Light solid lines show biexponential data fitting. Exponential relaxation times corresponding to two kinetic phases of denaturation are shown. B: Arrhenius plots, -ln k versus 1/T, for the two phases of reconstituted HDL (rHDL) denaturation. The values of k(T) (scattered symbols) determined from exponential fitting of the temperature jump (T-jump) data (such as those in A) are combined from three sets of experiments. The plots are approximated by linear functions (solid lines) that have similar slopes corresponding to activation energy $E_a = 30 \pm 7$ kcal/mol for each kinetic phase; the error in E_a determination reflects fitting errors and deviations among different data sets.

such kinetic CD data, $\Theta_{222}(t)$, recorded of apoC-I:DPPC disks in T-jumps from 25°C to 75–95°C. Similar data of apoC-I:DMPC disks could be fitted by single exponentials, suggesting single unfolding phase with activation energy (enthalpy) $E_a = 25 \pm 5$ kcal/mol (16, 17); however, the data in Fig. 2A could only be fitted by double exponentials, suggesting two kinetic phases of denaturation. The Arrhenius plots for these two phases were parallel, suggesting similar activation energy $E_a = 30 \pm 7$ kcal/mol (Fig. 2B).

To determine the physical origin of these two kinetic phases, we visualized particles at various stages of denaturation by negative staining EM (**Fig. 3**). DPPC-containing complexes were subjected to a T-jump to 75°C; sample aliquots taken after 5–180 min of incubation at 75°C were quickly cooled to 22°C and visualized by EM. Because apoC-I does not spontaneously clear DPPC even after prolonged incubation at $T_c = 41°C$ where protein-lipid association is fastest, rapid cooling from 80–22°C may not significantly affect the particle morphology observed by EM. EM data showed that incubation of intact disks at 80°C for 5–10 min (which corresponds to the exponential relaxation time τ_1 of the first kinetic phase) resulted in formation of larger particles that are probably small unilamellar vesicles (d = 25–40 nm, Fig. 3B), while incubation for 2 h (which corresponds to τ_2) and longer led to formation of much larger, possibly multilamellar, vesicles (d $\cong$ 100 nm, Fig. 3C). This suggests that the first kinetic phase involves partial protein unfolding, dissociation, and disk-to-vesicle fusion, whereas the second phase involves complete protein unfolding, dissociation, and further fusion into larger vesicles.

ApoC-I complexes with DSPC, POPC, or PLPC showed similar two-phase denaturation kinetics involving formation of progressively larger particles (CD and EM data not shown). In contrast, apoC-I complexes with DLPC (data not shown) or DMPC (16, 17) showed single-phase denaturation culminating in formation of multilamellar vesicles. Thus, apoC-I complexes with shorter-chain PCs (12–14 carbons) showed single-phase denaturation, whereas in similar complexes with longer-chain PCs (16–18 carbons, fully or partially saturated), two kinetic phases were resolved, yet fusion products of these complexes were similar. All complexes with apoA-I showed single-phase denaturation kinetics.

Effects of chain length in fully saturated PCs on rHDL stability

To assess relative stability of apoC-I complexes with fully saturated PCs containing 12–18 carbons, these complexes were heated and cooled at a constant rate of 11°C/h and CD melting data were recorded at 222 nm to monitor protein unfolding. The heating data showed large high-temperature shifts upon increasing acyl chain length (**Fig. 4A**), suggesting increased stability. To test this notion, we compared denaturation kinetics of different complexes; Figs. 4B, C show kinetic data recorded in T-jumps
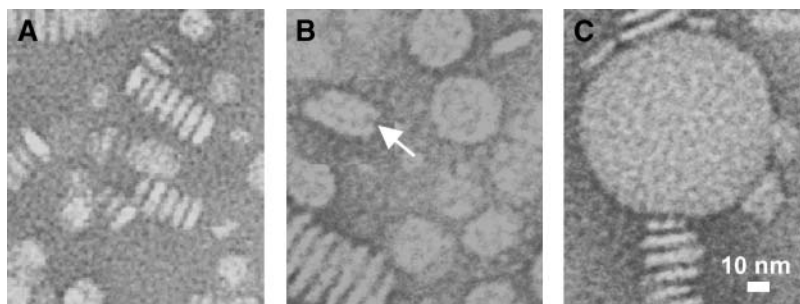

Fig. 3. Electron micrographs of apoC-I:dipalmitoyl phosphatidylcholine (DPPC) disks at various stages of heat denaturation. Intact disks (A) and disks after incubation at 75°C for τ_1=10 min (B) or $\tau_2 = 120$ min (C), whereas τ_1 and τ_2 are exponential relaxation times measured by CD in a T-jump to 75°C. White arrow in panel B shows a collapsed vesicle with characteristically rounded edges.
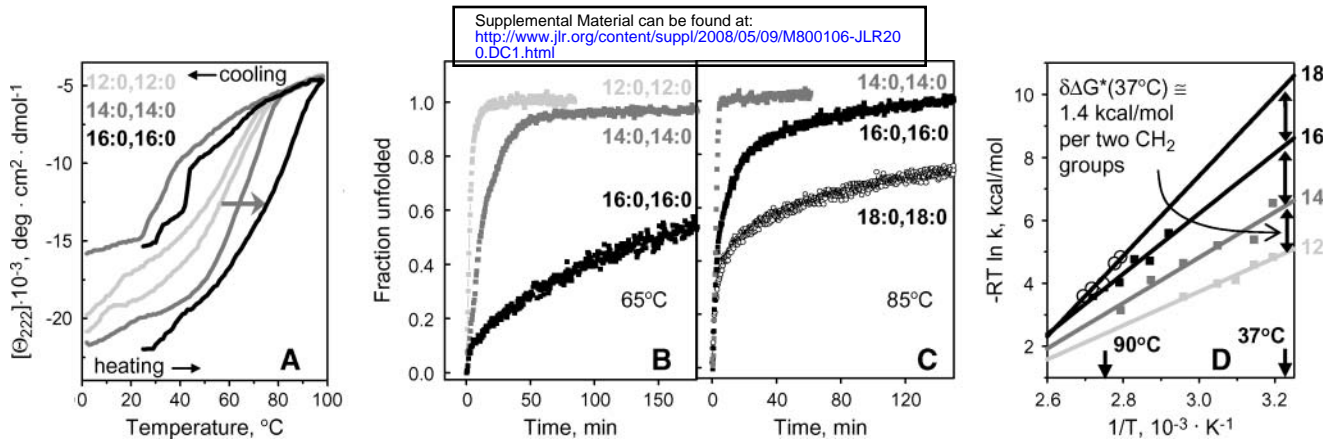
Acyl chain effects on rHDL stability 1755

Fig. 4. Effect of acyl chain length on thermal denaturation of apoC-I complexes with fully saturated phosphatidylcholines (PCs). Discoidal complexes of apoC-I (20 μg/ml protein in 5 mM Na phosphate, pH 7.7) with dilauroyl PC (DLPC) (light gray), dimyristoyl PC (DMPC) (gray), dipalmitoyl PC (DPPC) (black), or distearoyl PC (DSPC) (black open symbols) in 5 mM NaH_2PO_4, pH 7.7, were used. A: CD heating and cooling data, $\Theta_{222}(T)$, recorded at a scan rate of 11°C/h (the data for DSPC are not shown to avoid overlap). Shift in the heating curves upon increase in the acyl chain length is shown by the gray arrow. The hysteresis between the heating and cooling curves was addressed earlier (16, 17) and is a hallmark of a kinetically controlled transition with high free energy barrier for forward and reverse reaction. The hysteresis is reduced for shorter-chain DLPC, reflecting relative ease of spontaneous protein reconstitution with this lipid. B, C: Kinetic CD data, $\Theta_{222}(T)$, recorded in T-jumps to 65°C or 85°C (for complexes with PCs containing 12–16 or 14–18 carbons, respectively). The data are normalized to fraction unfolded (D) Arrhenius plots for apoC-I complexes with PCs differing in chain length. The plot for each complex was obtained from exponential approximation of the T-jump data such as those in Fig. 2A; for DPPC- and DSPC-containing particles, the first kinetic phase corresponding to disk fusion is shown. Linear extrapolation of the Arrhenius plots to 37°C (solid lines) suggests that increasing chain length by two CH_2 groups increases the kinetic disk stability by approximately 1.4 kcal/mol (double arrows).

to 65°C or 85°C. Slower protein unfolding was observed in complexes with longer-chain PCs, confirming their increased stability.

To quantify the chain length effects on the disk stability, $\Delta G^* = \Delta H^* - T\Delta S^*$, and its enthalpic component, $\Delta H^* \cong E_a$, we carried out Arrhenius analyses of the kinetic CD data. T-jump data recorded from each complex were approximated by exponential functions (solid lines in Fig. 2A), the unfolding rates k(T) were determined, and the Arrhenius plots, $-RT \ln k$ versus $1/T$, were obtained. For the complexes formed by longer-chain PCs, the Arrhenius plots for the first kinetic phase (corresponding to fusion of intact disks) were used for comparison. The results (Fig. 4D) show that chain length increase from 12 to 18 carbons leads to a gradual increase in the slope of the Arrhenius plot corresponding to an increase in the activation energy from $E_a = 20 \pm 5$ kcal/mol for apoC-I:DLPC to $E_a = 36 \pm 6$ kcal/mol for apoC-I:DSPC disks, or by approximately $\delta E_a \cong 5$ kcal/mol per two CH_2 groups (Table 1). Linear extrapolation of the Arrhenius plots to 37°C suggests that chain length increase by two CH_2 groups leads to increased kinetic stability by $\delta\Delta G(37°C) \cong 1.4$ kcal/mol (Fig. 4D, double arrows). Comparison with the value of δE_a suggests that this stabilization is dominated by enthalpy that must result from transient disruption of hydrophobic interactions involving fatty acyl chains during disk denaturation.

Effects of acyl chain length in complexes with other proteins

To test whether the binary complexes of fully saturated diacyl PCs with other apolipoproteins show similar chain length effects, we determined kinetic stability of such complexes with human apoA-I (**Fig. 5**) and apoA-II (data not

shown). The results, including melting data recorded by DSC and CD and kinetic T-jump data recorded by CD, clearly show that longer-chain PCs form more stable disks (Fig. 5). Earlier studies of DMPC complexes revealed that the rank order of the disk stability correlates with protein size, apoA-I > apoA-II$_{dimer}$ > apoA-II $_{mono}$ ≥ apoC-I (15). Similarly, other lipids (DLPC, DPPC, and DSPC) formed more stable complexes with apoA-I than with apoC-I. High stability of apoA-I complexes with DPPC and, particularly, DSPC limited quantitative analysis of their unfolding to a narrow high-temperature range (Fig. 5B illustrates slow denaturation of apoA-I:DPPC and apoA-I:DSPC complexes at 90°C), hampering accurate Arrhenius analyses and extrapolation to 37°C. Comparison of the unfolding rates of apoA-I complexes measured at 90°C showed that chain length increase by two CH_2 groups stabilizes the disks by approximately $\delta\Delta G^*(90°C) \cong 1.2$ kcal/mol (Fig. 5B, C). This is larger than the value $\delta\Delta G^*(90°C) \cong 0.7$ kcal/mol assessed for apoC-I complexes from the shifts in their Arrhenius plots at 90°C (Fig. 4D); this is consistent with a notion that more lipid molecules dissociate with each molecule of apoA-I as compared with apoC-I during disk denaturation (see Discussion). In summary, binary complexes of different proteins (apoC-I, apoA-I, apoA-II) and lipids (DLPC, DMPC, DPPC, DSPC) show a similar trend: longer-chain lipids form more stable disks.

Effects of acyl chain unsaturation on rHDL stability

Most PCs in plasma HDL have one or more double bonds in one of their fatty acyl chains. To test the effect of these double bonds on the disk stability, we analyzed denaturation kinetics of apoC-I complexes with POPC (16:0, 18:1) and PLPC (16:0, 18:2) that are abundant in human HDL (19). Comparison with length-matched fully
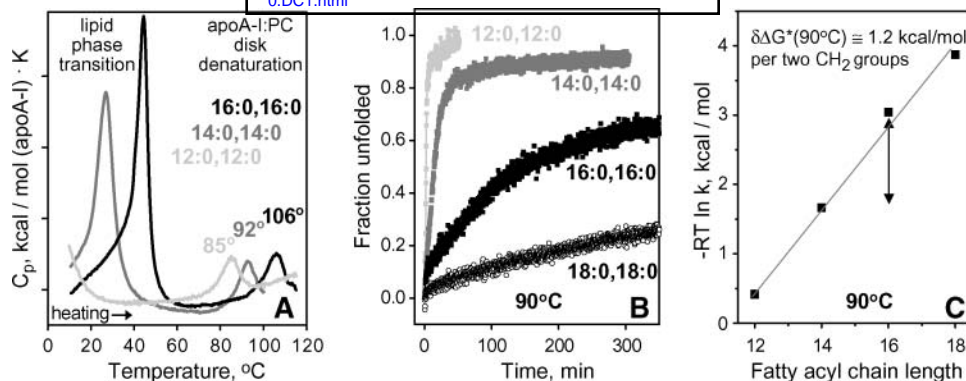
Fig. 5. Chain length effects on heat denaturation of apoA-I complexes with fully saturated diacyl PCs. A: Partial specific heat capacity $C_p(T)$ recorded upon heating of discoidal apoA-I complexes with DLPC, DMPC, or DPPC at a rate of 90°C/h. Low-temperature peaks are centered near T_c of the gel-to-liquid crystal lipid phase transition (Table 1), and high-temperature peaks are centered at the apparent temperature $T_{m,app}$ of the disk denaturation. Increase in $T_{m,app}$ with chain length increase suggests disk stabilization. B: Time course of protein unfolding upon disk denaturation at 90°C monitored in T-jumps by CD at 222 nm. Slower unfolding in complexes with longer-chain PCs indicates higher kinetic stability of these complexes. The unfolding rates k(90°C), which were determined from single-exponential fitting of the $\Theta_{222}(t)$ data, were used to obtain the plot in C. C: Kinetic disk stability $\Delta G^*(90°C) \sim -RT \ln k(90°C)$ as a function of chain length. The slope of the plot corresponds to disk stabilization by $\delta\Delta G^*(90°C) = 1.2$ kcal/mol upon chain length increase by two CH_2 groups (shown by double arrow).

saturated DPPC (16:0, 16:0) and DSPC (18:0, 18:0) shows that rHDL formed by cis-unsaturated PCs unfold faster and thus are less stable. For example, T-jumps to 60°C show faster protein unfolding in complexes with POPC or PLPC as compared with similar complexes with DPPC (**Fig. 6A**) or DSPC (that underwent little unfolding even after 6 h incubation at 60°C, data not shown). At higher temperatures, the differences in the unfolding rates among these complexes were less pronounced, as reflected in the
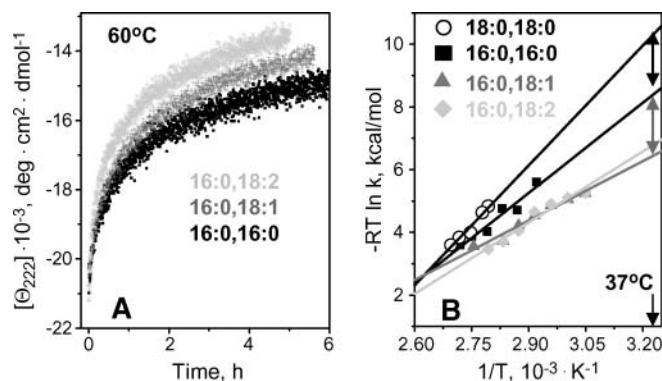
Arrhenius plots that intersect near 100°C. However, at lower temperatures, increasing differences among the Arrhenius plots indicate lower stability of lipoproteins formed by unsaturated PCs (Fig. 6B). Extrapolation of the Arrhenius plots to 37°C suggests that the stability of apoC-I:POPC disks is reduced by $\delta\Delta G^*(37°C) \sim$ 1.5 kcal/mol compared with DPPC disks, and by approximately 3 kcal/mol compared with DSPC disks (Fig. 6B, double arrows). Thus, the double bond in the oleic acid of POPC significantly destabilizes rHDL at near-physiologic temperatures. A large enthalpic contribution to this destabilization is evident from the comparison of the activation energies of the disk denaturation determined from the slopes of the Arrhenius plots, $E_a = 20 \pm 6$ kcal/mol for POPC, 30 ± 6 kcal/mol for DPPC, and 36 ± 5 kcal/mol for DSPC (Table 1). Therefore, the destabilizing effect of one *cis*-double bond in a fatty acyl chain is enthalpy driven.

Compared with monounsaturated POPC, complexes formed by diunsaturated PLPC showed only a small additional reduction in stability (Fig. 6A). The Arrhenius plots of these complexes partially overlapped (Fig. 6B) suggesting comparable disk stabilities, and the activation energies determined from these plots were similar, $E_a = 18 \pm 6$ kcal/mol for PLPC and 20 ± 6 kcal/ mol for POPC (Table 1). Therefore, the second double bond is only marginally destabilizing.

Effects of solvent ionic conditions

Both hydrophobic and electrostatic interactions significantly contribute to disk stability (23 and references therein). The latter may result from high content of charged residues (30–40%) in the exchangeable apolipoproteins and their characteristic radial distribution in class-A α-helices, with basic residues located in the low-dielectric environment at the lipid surface, which may alter
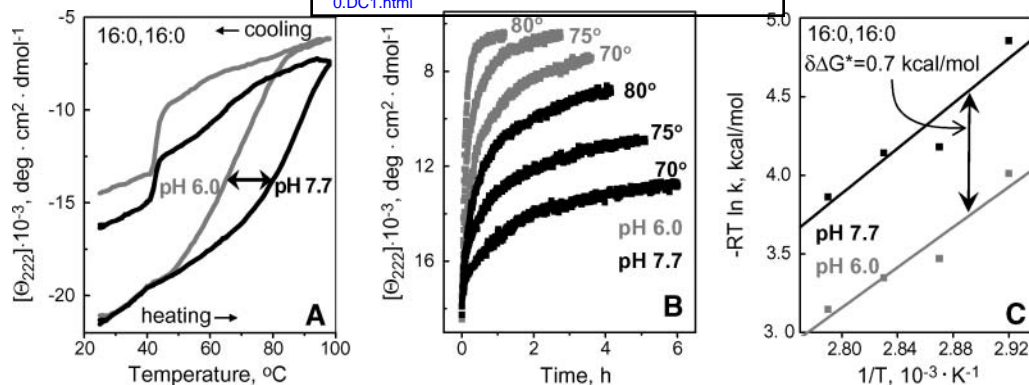

Fig. 6. Effect of fatty acyl chain unsaturation on the kinetic disk stability. Thermal unfolding kinetics of apoC-I complexes with diunsaturated PLPC (light gray), monounsaturated palmitoyl-oleoyl PC (POPC) (dark gray triangles), and fully saturated DPPC (black, filled squares) and DSPC (black open circles) was analyzed in T-jumps. A: Time course of heat denaturation monitored by CD at 222 nm in a T-jump to 60°C; the unfolding of apoC-I complexes with DSPC (not shown) is extremely slow at 60°C. B: Arrhenius plots for the 1st kinetic phase of disk denaturation. The plots for apoC-I complexes with POPC and palmitoyl-linoleoyl PC (PLPC) (dark and light gray) significantly overlap, suggesting comparable stability of these complexes at 37°C. Solid lines show linear fits; double arrows indicate differences in rHDL stability at 37°C.

Fig. 7. Effect of pH on thermal stability of apoC-I:DPPC disks. CD data at 222 nm were recorded of the disk samples (20 μg/ml protein in 5 mM Na phosphate buffer) at pH 7.7 (black) or pH 6.0 (gray). A: Melting data Θ_{222}(T) recorded at a scan rate of 11°C/h; arrow shows pH-induced shift in the heating curves. A steep increase in negative CD signal upon cooling to approximately 41°C, which is the phase transition temperature T_c of DPPC, reflects increase in the helix content of apoC-I upon lipid binding facilitated by the presence of lipid packing defects near T_c. B: T-jump data from 25°C to 70°C, 75°C or 80°C. C: Arrhenius plots, −RT ln k versus 1/T, for the 1st kinetic phase obtained from exponential fitting of the T-jump data in B; double arrow indicate pH-induced changes in the free energy barrier for disk denaturation, $\delta\Delta G^* = 0.7$ kcal/mol.

their pKs and amplify electrostatic interactions. Earlier, we showed the importance of electrostatic interactions in apoC-I:DMPC complexes (23); now we hypothesize that such interactions are different on disks of different thickness. To test this hypothesis, we analyzed the effects of pH and salt on the stability of apoC-I complexes with fully saturated PCs varying in chain length.

Effects of pH

Variations in pH from pH 5.8–8.5 showed no significant effects on the structure and stability of apoC-I complexes with DLPC (data not shown) or DMPC (23). In contrast, apoC-I complexes with DPPC and DSPC were destabilized at acidic pH, as suggested by the low-temperature shift by -15°C in the CD melting data of apoC-I:DPPC disks in 5 mM Na phosphate upon reduction in pH from pH 7.7 to 6.0 (**Fig. 7A**). Furthermore, kinetic T-jump data of these disks showed faster protein unfolding, and hence lower lipoprotein stability, at pH 6.0 as compared with pH 7.7 (Fig. 7B). Arrhenius analysis of these data (illustrated for the 1st kinetic phase in Fig. 7C) showed that reduction from pH 7.7 to 6.0 destabilizes the disks by $\delta\Delta G^* = -0.7$ kcal/mol. Similar destabilization was observed for apoC-I:DSPC disks (data not shown). Thus, in contrast to apoC-I complexes with DLPC and DMPC, similar complexes with DPPC and DSPC are destabilized at acidic pH.

To determine the pH dependence of this destabilization, we recorded kinetic CD data from apoC-I:DPPC or apoC-I:DSPC complexes in 5 mM Na phosphate buffer from pH 5.8 to 8.5 with increment of 0.2–0.3 pH. **Fig. 8A** shows such data of apoC-I:DPPC disks recorded at selected pH in T-jumps to 80°C. Exponential relaxation times $\tau_1 = 1/k_1$ for the first kinetic phase of disk denaturation determined from such data are plotted as a function of pH for apoC-I:DPPC and apoC-I:DSPC disks (Fig. 8B, C). The results show that the changes in the unfolding rates occur between pH 6.3 and 8.0 and follow an apparently normal titration with pK 7.2 (Fig. 8B, C).

Because apoC-I lacks His, the only group that has normal pK at near-neutral pH is N-terminal α-amino group. Even though other ionizable groups on rHDL may have anomalous pK, they are unlikely to account for the observed changes in disk stability near pH 7.2 (Fig. 8B, C). In fact, apolipoprotein lysines, which are located at the disk surface reportedly have pK ⩾ 8.4 that differ depending on the Lys microenvironment (26–28), and the pKs of Arg are expected to be even higher, hence titration of basic groups is unlikely to result in a narrow sigmoidal transition centered at pH 7.2 (Fig. 8B, C). Anomalous titration of the carboxyls also appears unlikely, because all acidic groups in apoC-I are located in the middle of the solvent-exposed polar helical face. Consequently, titration of α-NH₂ is the most likely cause for the observed pH

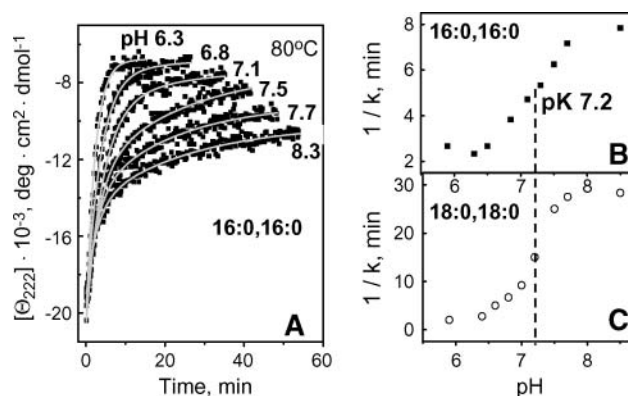**Fig. 8.** Effect of pH on thermal unfolding kinetics of apoC-I complexes with DPPC or DSPC. A: CD data of apoC-I:DPPC disks (20 μg/ml protein in 5 mM Na phosphate buffer) recorded at selected pH in T-jumps from 25–80°C. Relaxation time $\tau_1 = 1/k_1$ for the 1st kinetic phase obtained from exponential fitting of the T-jump data is plotted as a function of pH for apoC-I:DPPC (B) and apoC-I:DSPC disks (C). Plots in B and C are consistent with normal titration with pK 7.2 ± 0.1 (dashed line).

effect. To further test this notion, we analyzed the effects of pH on similar complexes containing a larger homologous protein, apoA-I (243 aa). Discoidal complexes of apoA-I with DMPC, DPPC, or DSPC are relatively small ($<$d$>$ $\cong$ 8–12 nm) and contain 2–3 protein molecules (8), whereas similar complexes with apoC-I (57 aa) are larger (d = 12–19 nm) and contain approximately 15–20 protein molecules. Thus, the effect of the N-terminal titration on the disk stability is expected to be greatly diminished in rHDLs containing apoA-I as compared with apoC-I. Thermal denaturation data at pH 5.9–8.3 showed no significant effects of pH on the stability of apoA-I complexes with any lipid explored (data not shown). This result is consistent with the notion that the effects of pH observed in apoC-I:DPPC and apoC-I:DSPC disks (Fig. 6, 7) may, at least in part, result from titration of multiple copies of the N-terminal α-amino group.

Why are the pH effects observed in apoC-I complexes with longer- (DPPC and DSPC) but not shorter-chain PCs (DLPC and DMPC)? Longer-chain PCs form thicker disks (Table 1) that likely have larger apolar area around their perimeter in contact with the protein. As a result, the protein molecules on these disks, including their N-terminal groups, may form more extensive contacts with the lipid; hence the titration of these groups affects the disk stability. In comparison, thinner disks formed by shorter-chain PCs may have N-terminal segments dissociated from the lipid; hence the titration of the NH$_2$ groups has no detectable effect on the disk stability. A small ($\sim$7%) increase in the α-helix content of apoC-I observed upon chain length increase from 12 to 18 carbons (CD spectra not shown) is consistent with this notion.

Effects of salt

Earlier analysis of ionic strength effects on the wild-type and mutant apoC-I:DMPC disks and other model and plasma HDLs revealed a general trend: salt stabilizes less stable rHDLs, probably due to ionic screening of unfavorable electrostatic interactions, but destabilizes more stable rHDLs in which electrostatic interactions are better optimized (23, 25). To further test this notion, we assessed the effects of physiologic salt concentrations on the stability of apoC-I:DPPC disks at pH 6.0–7.7. At pH 7.7 (where the disks are more stable), no significant effect of salt on their thermal denaturation was detected (CD data not shown). In contrast, at pH 6.0, increase in NaCl concentration from 0–150 mM in 5 mM Na phosphate buffer stabilized the disks, as evident from the high-temperature shift in the heating data by nearly 10°C and from deceleration of the lipoprotein denaturation observed in T-jumps (**Fig. 9A, B**). Arrhenius analysis of the apoC-I:DPPC disk denaturation at pH 6.0 (not shown) suggests that this salt-induced stabilization amounts to δΔG* = 0.4 kcal/mol. A similar stabilizing effect of NaCl at pH 6.0 but not at pH 7.7 was observed in apoC-I:DSPC disks (data not shown). These results further support the inverse correlation between the effect of salt and rHDL stability (23).
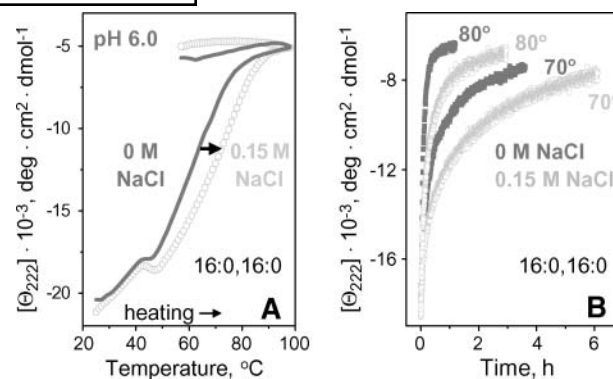

Fig. 9. Effect of salt on thermal stability of apoC-I:DPPC disks at pH 6.0. A: CD melting data recorded at 11°C/h scan rate. B: Kinetic CD data $\Theta_{222}(t)$ recorded in T-jumps to 70°C or 80°C. Solvent conditions are 5 mM Na phosphate buffer in the absence (dark gray) or presence (light gray) of 150 mM NaCl.

DISCUSSION

Role of hydrophobic interactions in kinetic rHDL stability

This work provides the first kinetic analysis of the effects of lipid composition on lipoprotein stability. The results reveal that stability of binary discoidal protein:PC complexes increases with increasing acyl chain length and saturation (Figs. 4–6 and Table 1). Even though some of these complexes show monoexponential unfolding kinetics (all apoA-I complexes and apoC-I complexes with DLPC and DMPC) while others can be fitted by two exponents (apoC-I complexes with DPPC, DSPC, POPC and PLPC), the results for denaturation of intact disks (which clearly corresponds to the first exponential phase, Figs. 2 and 3) can be directly compared for all these lipids. For apoC-I complexes with fully saturated PCs, chain length increase by two CH$_2$ groups leads to an increase in the free energy of the disk stability by δΔG*(37°C) $\cong$ 1.4 kcal/mol and in its enthalpic component by δE$_a$ $\cong$ 5 kcal/mol (Fig. 4D), suggesting enthalpic stabilization. Similarly, comparison of rHDL formed by fully saturated DPPC and DSPC with their length-matched unsaturated analogs, POPC and PLPC, shows that higher stability of the complexes formed by fully saturated lipids is an enthalpic effect (Table 1). This effect results from transient disruption of hydrophobic lipid-lipid and lipid-protein interactions (which are more extensive in longer and in more saturated acyl chains) during protein dissociation and lipoprotein fusion (Fig. 1). Furthermore, increase in disk stability by δΔG*(25°C) $\cong$ 1.5 kcal/mol per two CH$_2$ groups suggests that, for rHDL containing DMPC (14:0, 14:0) in a bilayer conformation, the contribution from the interactions involving acyl chains to ΔG* is approximately 14 × 1.5 kcal/mol $\cong$ 21 kcal/mol. This is comparable to the estimated kinetic stability of apoC-I:DMPC disks, ΔG*(25°C) $\cong$ 18–24 kcal/mol (17). Thus, hydrophobic interactions involving fatty acyl chains provide the major contribution to rHDL stability. An additional contribution comes from electrostatic interactions among protein charged groups, as evident from distinct effects of pH and salt (Figs. 7–9).

Cooperative unit and transition state in rHDL denaturation

In contrast to calorimetric enthalpy that is determined on the molar basis of a macromolecule, energetic parameters measured by spectroscopy, such as effective enthalpy $\Delta H^* \cong E_a$ or free energy barrier ΔG^*, are determined per mole of cooperative unit involved in the transition, and hence provide insight into the nature of this unit. Our observation that rHDL disks with similar protein and lipid composition but different diameters may have similar ΔG^* and E_a (see supplemental data) implies that the cooperative unit in rHDL denaturation may not comprise the whole particle (otherwise, particles with larger diameters would have had larger E_a). Furthermore, an increase in ΔG^* and E_a with increasing protein size, A-I > A-II$_{dimer}$ > A-II$_{mono}$ ≥ C-I (15), suggests (but does not prove) that cooperative unit involves one protein molecule. Specifically, disulfide reduction in apoA-II:DMPC disks, which converts apoA-II dimer into monomer without altering the disk structure or protein conformation, greatly reduces disk stability ΔG^* and activation energy of disk denaturation E_a (15), suggesting that the two monomers within the dimer form a single cooperative unit only if they are covalently linked. This is consistent with the notion that only one protein molecule is involved in cooperative dissociation from the simple binary protein:lipid complexes used in our work. In more complex systems, such as discoidal or spherical HDL containing both apoA-I and apoA-II, cooperative unit may potentially involve more than one protein molecule; more studies are required to test this notion.

The results reported here reveal that ΔG^* and E_a increase with increasing acyl chain length and saturation (Figs. 4–6, Table 1); therefore, acyl chains form an integral part of the cooperative unit. Taken together, our results suggest that the cooperative unit in rHDL denaturation comprises a lipidated protein molecule that dissociates from rHDL, eventually leading to particle fusion (Fig. 1). In this model, the rate-limiting step in HDL denaturation is dissociation of lipidated apolipoprotein; the activation energy (enthalpy) $\Delta H^* \cong E_a$ arises from transient disruption of protein-lipid and lipid-lipid interactions during such a dissociation, the activation entropy ΔS^* arises from transient solvent exposure of apolar lipid and protein moieties, and their difference determines kinetic rHDL stability, $\Delta G^* = \Delta H^* - T\Delta S^*$.

This model helps interpret the observed increase in disk stability by $\delta\Delta G^*(25°C) \cong 1.5$ kcal/mol upon chain length increase by CH_2 groups (Table 1). Importantly, the value of $\delta\Delta G^*$ pertains to mole of cooperative unit [that, we propose, comprises one protein and several lipid molecules (Fig. 1)]; hence, this value has to be divided among several molecules. Comparison with the free energy of transfer of two CH_2 groups from hydrophobic to aqueous environment at 25°C (1.7 kcal/mol) (29) suggests that the lipid molecules in the cooperative unit are only partially solvent exposed in the transition state. This is physically plausible because the packing of the protein and lipid molecules within the cooperative unit partially screens them from the solvent.

Correlation between disk stability and cell cholesterol efflux

Increase in the kinetic stability of rHDL with increasing acyl chain length was observed not only in apoC-I:PC complexes but also in similar complexes with other exchangeable apolipoproteins such as human apoA-I (Fig. 5). This enables direct comparison of our results with the existing cholesterol efflux data using similar binary complexes of apoA-I and diacyl PCs. Studies by Davidson et al. (13) of apoA-I complexes with DMPC, DPPC, DSPC and their unsaturated analogs showed that shorter-chain and unsaturated PCs form more efficient acceptor particles for unesterified cholesterol at 37°C. This was attributed to differences in the lipid phase (gel or liquid crystalline) formed at near-physiologic temperature, the liquid phase reportedly forming a better cholesterol acceptor due to its increased fluidity (13). Although highly plausible, this explanation did not address the differences among the PCs forming similar phase at 37°C. Correlation of functional studies by Davidson et al. (13) with our kinetic stability studies using apoC-I and apoA-I complexes with similar lipids suggests another explanation: shorter-chain and/or unsaturated PCs form less stable rHDL with lower free energy barrier ΔG^* for lipoprotein remodeling (Figs. 4–6, Table 1). We propose that this reduced global stability facilitates transient opening of the lipoprotein surface thereby accelerating cholesterol insertion.∎

REFERENCES

1. Fielding, C. J., and P. E. Fielding. 1995. Molecular physiology of reverse cholesterol transport. *J. Lipid Res.* **36:** 211–228.
2. von Eckardstein, A., J. R. Nofer, and G. Assman. 2001. High density lipoproteins and arteriosclerosis. Role of cholesterol efflux and reverse cholesterol transport. *Arterioscler. Thromb. Vasc. Biol.* **21:** 13–27.
3. Barter, P. J. 2002. Hugh Sinclair lecture: the regulation and remodeling of HDL by plasma factors. *Atheroscler. Suppl.* **3:** 39–47.
4. Kontush, A., S. Chantepie, and M. J. Chapman. 2003. Small, dense HDL particles exert potent protection of atherogenic LDL against oxidative stress. *Arterioscler. Thromb. Vasc. Biol.* **23:** 1881–1888.
5. Mishra, V. K., G. M. Anantharamaiah, J. P. Segrest, M. N. Palgunachari, M. Chaddha, S. W. Sham, and N. R. Krishna. 2006. Association of a model class A (apolipoprotein) amphipathic alpha helical peptide with lipid: high resolution NMR studies of peptide. lipid discoidal complexes. *J. Biol. Chem.* **281:** 6511–6519.
6. Davidson, W. S., and T. B. Thompson. 2007. The structure of apolipoprotein A-I in high density lipoproteins. *J. Biol. Chem.* **282:** 22249–22253.
7. Rye, K. A., and P. J. Barter. 2004. Formation and metabolism of

prebeta-migrating, lipid-poor apolipoprotein A-I. *Arterioscler. Thromb. Vasc. Biol.* **24:** 421–428.

8. Jonas, A., N. L. Zorich, K. E. Kézdy, and W. E. Trick. 1987. Reaction of discoidal complexes of apolipoprotein A-I and various phosphatidylcholines with lecithin:cholesterol acyltransferase. Interfacial effects. *J. Biol. Chem.* **262:** 3969–3974.

9. Jonas, A. 1986. Reconstitution of high-density lipoproteins. *Methods Enzymol.* **128:** 553–582.

10. Pownall, H. J., Q. Pao, and J. B. Massey. 1985. Isolation and specificity of rat lecithin: cholesterol acyltransferase: comparison with the human enzyme using reassembled high-density lipoproteins containing ether analogs of phosphatidylcholine. *Biochim. Biophys. Acta.* **833:** 456–462.

11. Sparks, D. L., W. S. Davidson, S. Lund-Katz, and M. C. Phillips. 1993. Effect of cholesterol on the charge and structure of apolipoprotein A-I in recombinant high density lipoprotein particles. *J. Biol. Chem.* **268:** 23250–23257.

12. Davidson, W. S., S. Lund-Katz, W. J. Johnson, G. M. Anantharamaiah, M. N. Palgunachari, J. P. Segrest, G. H. Rothblat, and M. C. Phillips. 1994. The influence of apolipoprotein structure on the efflux of cellular free cholesterol to high density lipoprotein. *J. Biol. Chem.* **269:** 22975–22982.

13. Davidson, W. S., K. L. Gillotte, S. Lund-Katz, W. J. Johnson, G. H. Rothblat, and M. C. Phillips. 1995. The effect of high density lipoprotein phospholipid acyl chain composition on the efflux of cellular free cholesterol. *J. Biol. Chem.* **270:** 5882–5890.

14. Parks, J. S., K. W. Huggins, A. K. Gebre, and E. R. Burleson. 2000. Phosphatidylcholine fluidity and structure affect lecithin:cholesterol acyltransferase activity. *J. Lipid Res.* **41:** 546–553.

15. Jayaraman, S., D. L. Gantz, and O. Gursky. 2005. Kinetic stabilization and fusion of discoidal lipoproteins containing human apoA-2 and DMPC: Comparison with apoA-1 and apoC-1. *Biophys. J.* **88:** 2907–2918.

16. Benjwal, S., S. Jayaraman, and O. Gursky. 2007. Role of secondary structure in protein-phospholipid surface interactions: reconstitution and denaturation of apolipoprotein C–I:DMPC complexes. *Biochemistry.* **46:** 4184–4194.

17. Gursky, O., Ranjana, and D. L. Gantz. 2002. Complex of human apolipoprotein C-1 with phospholipid: Thermodynamic or kinetic stability? *Biochemistry.* **41:** 7373–7384.

18. Mehta, R., D. L. Gantz, and O. Gursky. 2003. Human plasma high-density lipoproteins are stabilized by kinetic factors. *J. Mol. Biol.* **328:** 183–192.

19. Skipski, V. P. 1972. *In*: Blood Lipids and Lipoproteins. Quantitation, Composition and Metabolism. G. J. Nelson, editor. Wiley–Interscience, New York, pp. 471–483.

20. Cullis, P. R., and M. J. Hope. 1991. *In*: Biochemistry of Lipids, Lipoproteins and Membranes. D. E. Vance and J. E. Vance, editors. Elsevier, p. 17.

21. Jong, M. C., M. H. Hofker, and L. M. Havekes. 1999. Role of ApoCs in lipoprotein metabolism: functional differences between ApoC1, ApoC2, and ApoC3. *Arterioscler. Thromb. Vasc. Biol.* **19:** 472–484.

22. Shachter, N. S. 2001. Apolipoproteins C–I and C–III as important modulators of lipoprotein metabolism. *Curr. Opin. Lipidol.* **12:** 297–304.

23. Benjwal, S., S. Jayaraman, and O. Gursky. 2005. Electrostatic effects on the kinetic stability of model discoidal high-density lipoproteins. *Biochemistry.* **44:** 10218–10226.

24. Mehta, R., D. L. Gantz, and O. Gursky. 2003. Effects of mutations on the reconstitution and kinetic stability of discoidal lipoproteins. *Biochemistry.* **42:** 4751–4758.

25. Jayaraman, S., D. L. Gantz, and O. Gursky. 2006. Effects of salt on thermal stability of human plasma high-density lipoproteins. *Biochemistry.* **45:** 4620–4628.

26. Sparks, D. L., M. C. Phillips, and S. Lund-Katz. 1992. The conformation of apolipoprotein A-I in discoidal and spherical recombinant high density lipoprotein particles. 13C NMR studies of lysine ionization behavior. *J. Biol. Chem.* **267:** 25830–25838.

27. Lund-Katz, S., M. Zaiou, S. Wehrli, P. Dhanasekaran, F. Baldwin, K. H. Weisgraber, and M. C. Phillips. 2000. Effects of lipid interaction on the lysine microenvironments in apolipoprotein E. *J. Biol. Chem.* **275:** 34459–34464.

28. Zaiou, M., K. S. Arnold, Y. M. Newhouse, T. L. Innerarity, K. H. Weisgraber, M. L. Segall, M. C. Phillips, and S. Lund-Katz. 2000. Apolipoprotein E–low density lipoprotein receptor interaction. Influences of basic residue and amphipathic alpha-helix organization in the ligand. *J. Lipid Res.* **41:** 1087–1095.

29. Tanford, C. The Hydrophobic Effect, John Wiley, New York, 1980.